Article

Effects of Reduced Graphene Oxide (rGO) at Different Concentrations on Tribological Properties of Liquid Base Lubricants

Jankhan Patel and Amirkianoosh Kiani *

Silicon Hall: Micro/Nano Manufacturing Facility, Faculty of Engineering and Applied Science, University of Ontario Institute of Technology (UOIT), Oshawa, ON L1H7K4, Canada; jankhankumarnayankumar.patel@uoit.net

* Correspondence: amirkianoosh.kiani@uoit.ca; Tel.: +1-(905)-721-8668 (ext. 5730)

Abstract: In this study, reduced graphene oxide (rGO) nano platelets were used as an additive to enhance friction and wear properties of oil-based lubricants by preparing three samples at 0.01% *w/w*, 0.05% *w/w*, and 0.1% *w/w* concentrations. To analyze the direct effect of rGO nano platelets on tribological properties, 99.9% pure oil was used as a liquid lubricant. A comparative tribological study was done by performing a ball-on-disk wear test in situ under harsh conditions, which was further analyzed using a non-contact 3D optical profilometer. Morphological evaluation of the scar was done using transmission and scanning electron microscopy (TEM, SEM) at micro and nano levels. The lubricants' physical properties, such as viscosity and oxidation number, were evaluated and compared for all samples including pure oil (control sample) as per ASTM standards. Findings of all these tests show that adding rGO nano platelets at 0.05% *w/w* showed significant reduction in friction at high speed and in wear up to 51.85%, which is very promising for increasing the life span of moving surfaces in machinery. Oxidation and viscosity tests also proved that adding rGO nano platelets to all samples does not sacrifice the physical properties of the lubricant, while it improves friction and wear properties.

Keywords: friction; wear; reduced graphene oxide (rGO)

1. Introduction

The sustainability of rotating and moving parts in machines plays an important role in production costs. For example, wear in parts as a result of improper lubrication or tribological practices can damage production capabilities by increasing maintenance costs, machine down time and part replacement costs. Statistical results show major costs associated with wear range from 20% to 55% for industrial sectors such as transportation, manufacturing, energy, and residential [1]. However, wear and friction play positive roles in applications such as material removal processes and mining. In general, to utilize the pros and cons of friction and wear, researchers proposed different methods for modifying viscosity, friction, wear, oxidation, and detergent capabilities of the lubricants [2].

Advancement in nanomaterial manufacturing capabilities has opened up new opportunities for enhancement of lubricant properties by adding various nanomaterials such as Fe, Cu, Co, HBN, onion-like carbon (OLC), and fullerene at different concentrations and morphologies [2–5]. Tribological and physical properties of lubricants modified by nanoadditives vary according to the size, shape, number of layers (for 2D nanoadditives), surface area, mechanical properties and chemical composition of such additives. Among all these materials, carbon-based nanoadditives have attracted much attention in applications such as energy storage, manufacturing and biomedical device fabrication.

Due to their widespread use in different fields, a great deal of research has been conducted to improve the manufacturing capabilities of carbon-based nanomaterials on wide-ranging characteristics that can be tuned for different applications. These characteristics are directly related to factors such as defects in crystalline structures, morphology and surface area, electrical and thermal conductivity, optical behavior, molecular specification, number of layers, and uniformity of the carbon-based nanomaterials [6].

Graphene, one of the emerging carbon allotropes, has been shown to possess excellent mechanical, thermal, electrical, and optical properties. As a result, it has been used for numerous applications such as storing energy, electronics, opto-electronics, sensing applications, and many more [7–14]. Previous studies show that graphene particles can mitigate metal-to-metal contact and enhance wear behaviors of moving and mating parts. Graphene nano platelets with high surface areas have only a few layers (two to ten layers), and the weak van der Waals forces between these layers generate material lubricity, which can shear under the loading conditions [15]. However, low dispersibility of graphene in liquid-based lubricants is considered a main challenge. Because of their high surface area, graphene nano platelets can start conglomerating in the lubricant shortly after mixing with the liquid lubricants [16]. This problem can be resolved by using different surface modifications of the graphene particles; however, these modifications have high environmental and ecological costs.

Graphene oxide (GO) is another carbon allotrope that has recently found more applications in different sectors including lubrications and tribology. However, graphene oxide (GO), can also generate defects in sp3 bonding and can form oxygen functional groups while mixing with organic lubricants. Graphene oxide can be converted to reduced graphene oxide (rGO) by different reduction methods such as chemical, thermal reduction and hydrogen plasma treatment [17–24]. Each method can produce reduced graphene oxides, which are varied as per C/O ratio, defects in layers and concentration of oxygen groups between the layers. Recently, reduced graphene oxide has been used in applications such as gas sensing, transparent electrodes, and energy storage device fabrication. More applications for rGO nano platelets are being evaluated because of cheaper cost and fewer morphology defects in 2D forms of rGO [25].

In this study, we investigated the tribological effects of highly reduced graphene oxide (H-rGO) nano platelets as additives to mineral base oil. Highly-reduced graphene oxide has fewer oxygen groups present between the micro layers, which can allow spacing between the surfaces to accommodate the lubricant. With that in mind, rGO was tested using a tribometer in situ to perform a comparative study. Anti-oxidation, particle spectroscopy, and kinematic viscosity tests were also evaluated. The results shown in this study can lead to new applications for rGO in tribology and lubrication science and engineering [25].

2. Method

2.1. Materials

Reduced graphene oxide nano platelets (Digi-Key Electronics, Thief River Falls, MN, USA, product #: 1767-1014-ND) were manufactured using a modified Hummers' method with a single sealed jar [26]. This was further evaluated as a hydrophobic and conductive material which contains 85% carbon. The bulk density of the material was calculated as 2.0 mg/cm^3. To analyze the actual effect of a nano additive on a nano lubricant, pure base oil was used, provided by Petro Canada (Mississauga, ON, Canada, Purity 2204-#72623-87-1: 99.9% pure, % aromatics: 0.1 with sulfur <10 ppm). The base oil was HT purified and classed as Group II and Group III lubricants as per American Petroleum Institute (API) standards. Pure crystal clear base oil (hydrotreated neutral base oil) provides users the flexibility to prepare different combinations of required properties such as viscosity modifiers, friction modifiers and wear resistive lubricants. The base oil's pour point of −18 °C and flash point of 240 °C were obtained from the material data sheet provided by Petro Canada. In addition, its low temperature

capability and high viscosity index properties will always try to reduce the temperature fluctuation, which allows the lubricant to maintain a thin lubrication film between solid contacts.

2.2. Sample Preparation

For dispersion of graphene nano platelets into the lubricant, high shear force is required. To achieve this, a mechanical mixture was used for 20 minutes to shear the rGO platelets into the lubricant, followed by 10 minutes of ultra-sonication. Three concentrations were then prepared, as shown in Table 1, having different nano additive concentrations of 0.0 wt % (base oil), 0.01 wt %, 0.05 wt %, and 0.1 wt %, without any surface modification of reduced graphene oxide. Figure 1 also shows the difference between the samples immediately after preparation (A) and after keeping it in steady state for 45 days (B). Visual inspection revealed that for S-1 and S-2 concentrations, there is no significant gravitational effect on the particles' precipitation. However, for the higher concentrations it seems that particles started conglomerating and were deposited on the bottom surface of the plastic container. This illustrates that for concentrations higher than 0.1% w/w, suspension additives are required for the proper amalgamation of particles in the nano lubricant.

Table 1. Sample characterization of four different concentrations including base oil (error: $\pm 0.005\%$).

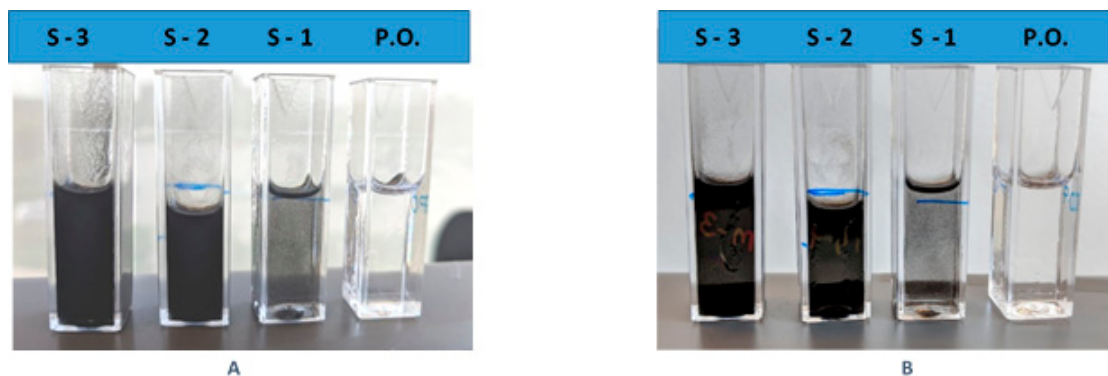| Sample Identification	Concentration
Pure Oil	No additive (99.9% pure)
Sample-1(S-1)	0.01% w/w nano additive
Sample-2(S-2)	0.05% w/w nano additive
Sample-3(S-3)	0.1% w/w nano additive

Figure 1. Four samples of reduced graphene oxide. (**A**) Samples after mechanical mixing and ultra-sonication, (**B**) Samples kept in steady state condition for 45 days.

2.3. Sample Characterization

2.3.1. TEM and SEM Analysis

As rGO aggregated and crumpled very closely to each other, it was difficult to investigate them under TEM. For preprocessing, rGO powder was poured in the mold, which was then filled with spur epoxy resin. After keeping it overnight in the oven at 65 °C to get it polymerized, 90 nm thick slices were cut using the diamond knife on a Leica UC7 ultramicrotome. The section was imaged using an FEI Tecnai 20 transmission electron microscope (TEM) (SickKids, Toronto, ON, Canada). To understand the worn surface morphology under high magnification, a Quanta 3D scanning electron microscope (SEM) was used at 120 magnification and 500 μm size (York University Microscopy Lab, Toronto, ON, Canada).

2.3.2. Raman Spectroscopy

Chemical composition of reduced graphene oxide was studied using Raman spectroscopy (the machine used was a Renishaw Imaging microscope system 2000, located in the Raman Lab at UOIT, ON, Canada). Additionally, the ratio of intensity at D band and G band was calculated to find the graphitic disorder and correlate with the mechanical properties of the additives.

2.3.3. FTIR

A Fourier transform infrared spectroscopy test was conducted to understand the wide range of particle sizes in the nanolubricant (Kinectrics Inc., Toronto, ON, Canada). A thin film of the material was placed on a KBr plate to generate the resulting spectrum. All the particles were characterized according to size as per ASTM D7619, D7647, and ISO-4 standards. The machine was examined using reference polystyrene film before performing the test. All the samples were agitated as per ASTM guidelines before performing tests.

2.3.4. Viscosity

Viscosity is an important physical property of lubricants, and to study the change in the viscosity due to nano additives at 40 °C and at 100 °C, a kinematic viscosity test was performed as per ASTM D445 (Kinectrics Inc., Toronto, ON, Canada). The average time was calculated for the lubricant to flow in the capillary tube under gravity. The product of the calculated time and the calibration constant of the viscometer gave values at 40 °C and 100 °C. Using the standard formula, the viscosity index was calculated.

2.3.5. RPVOT

The life of a lubricant can be determined using different methods such as odor, visual inspection, FTIR and oxidation time. However, while transforming graphene oxide into its reduced form, oxygen particles remain in the lattice. To identify the change in resistance to oxidation due to nano particles, a rotating pressure vessel oxidation test (RPVOT) was conducted as per ASTM D2272, and resistivity was measured to understand contaminants in the oil using ASTM D1169 (Kinectrics Inc., Toronto, ON, Canada). In the test specimen, a water and copper catalyst was placed with sample oil that had antioxidants. However, the antioxidants were consumed after a time and oil started reacting with the oxygen and reducing the pressure of the apparatus. The total time in minutes was counted from the beginning of the experiment to the pressure drop in the apparatus. The test was performed in the presence of oil, water, heat, and copper catalyst in a closed container at 90 psi and the temperature was elevated to 150 °C. For comparative analysis, the time was calculated to the drop in pressure to 14.5 psi in the chamber.

2.3.6. Ball-on-Disk Test

To understand the wear preventive characteristics of the lubricants, a ball-on-disk instrument (TRB181002-36-D at Nanovea, CA, USA) was used to test all four samples in the same condition. A schematic view of the ball-on-disk apparatus is shown in Figure 2. The covalent organic framework (COF) was obtained in situ. To calculate wear rate and surface roughness, a 3D profilometer (T-14-0133, Nanovea Inc., Irvine, CA, USA) was used. The motor of the tribometer was integrated with self-turning and all-time calibration capabilities to generate data precisely. A 6mm diameter ball indenter made from SS440C was held in the load arm. The 50 mm diameter disk was made from AISI-316-L stainless steel (C-0.023, Si- 0.40, Mn-1.59, P-0.037, S- 0.027, Cr-16.55, Mo-2.06, Ni-10.20, Co-0.20, N-0.0350, Cu-0.47). After the disk was machined, it was taken to the polisher (Nano 2000) and polished to less than 0.1 µm surface roughness.
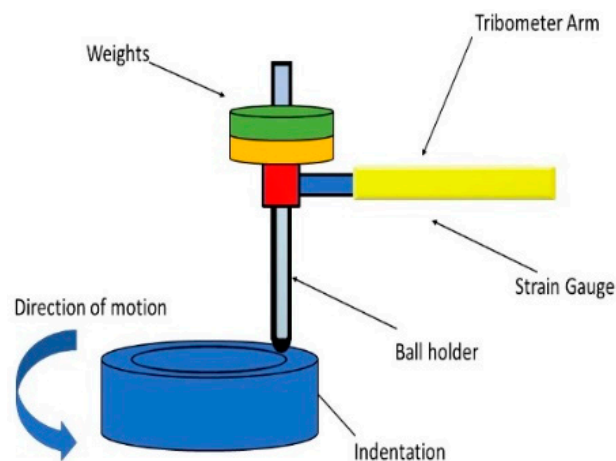
Figure 2. Ball-on-disk wear tester.

The tribometer was cleaned ultrasonically to ensure no nano particles would stick before the next test. Before running the tests, a counter weight to the arm was placed to ensure the arm and ball holder did not interfere with the load in the initial condition. Once the ball and disk were ready, a 30 N weight was placed on the arm of the ball holder (Table 2). Disk speed was increased logarithmically from 0.01 to 150 RPM. Each test was conducted for 20 minutes' duration and 312 revolutions of the disk. In addition, the temperature was maintained at 24 °C, and humidity was kept at 40%. The radius of the wear track was 10mm. A strain gauge sensor was placed on the load arm to gain data about friction with the revolution. To find comparative data about wear, the volume of lost material was measured using hole area analysis on the worn surface, and the obtained data were used to calculate wear. Values for wear and surface roughness (Sa and Sz) have been measured according to the ISO 25178 (Nanovea, CA, USA).

Table 2. Test parameters used for ball-on-disk test.

Test Parameters	Unit Value
Load	30 N
Test duration	20 min
Speed	0.01–150 RPM
Ramp type	Logarithmic
Radius	10 mm
Revolution	312 Revolution
Ball material	SS440C
Ball diameter	6 mm

2.4. Statistical Analysis

Statistical analysis was done using Microsoft Excel to ensure authenticity of the results. A minimum of three measurements were taken to obtain the values. Average values are shown with error bar marked on the graph, which represents the standard deviation.

3. Results and Discussion

3.1. Reduced Graphene Oxide Characterization

Transmission electron microscopy (TEM) at 50,000× magnification revealed that reduced graphene nano platelets aggregated randomly, as shown in Figure 3. The magnified view shows that few layers of rGO are attached in the hexagonal lattice. The rGO was evaluated as very fluffy and lightweight nano powder. Multiple layers of rGO were identified, as shown by the arrows in the 150,000× magnified view. Due to fine nano particles, rGO was able to provide high surface area compared to graphene

oxide, and this can be used to accelerate the nano platelets' penetration into the mating surfaces and enhance tribological properties.
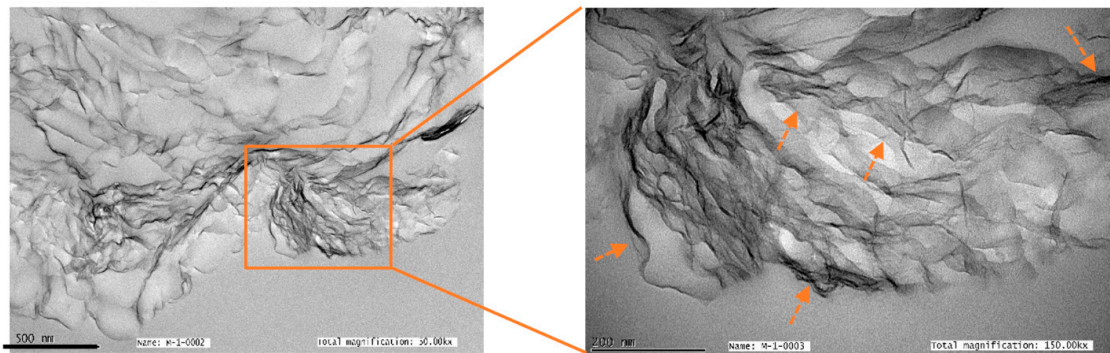

Figure 3. TEM images of reduced graphene oxide under $50,000\times$ and $150,000\times$ magnification.

Large particles can damage the filter of a hydraulic system, which can lead to inefficient performance. In order to investigate rGO particle size, an FTIR test was conducted. FTIR test results show the total number of particles per 1 ml. As shown in Figure 4, most of the nano particles range from 4 μm to 70 μm in size. Smaller particle sizes can breach between the surfaces and reduce wear and friction. It is necessary to consider particle size and filtering class in future applications as some larger particles would be filtered out in lubricant cleanliness of the 16/14/12 or better class (according to ISO 4406).
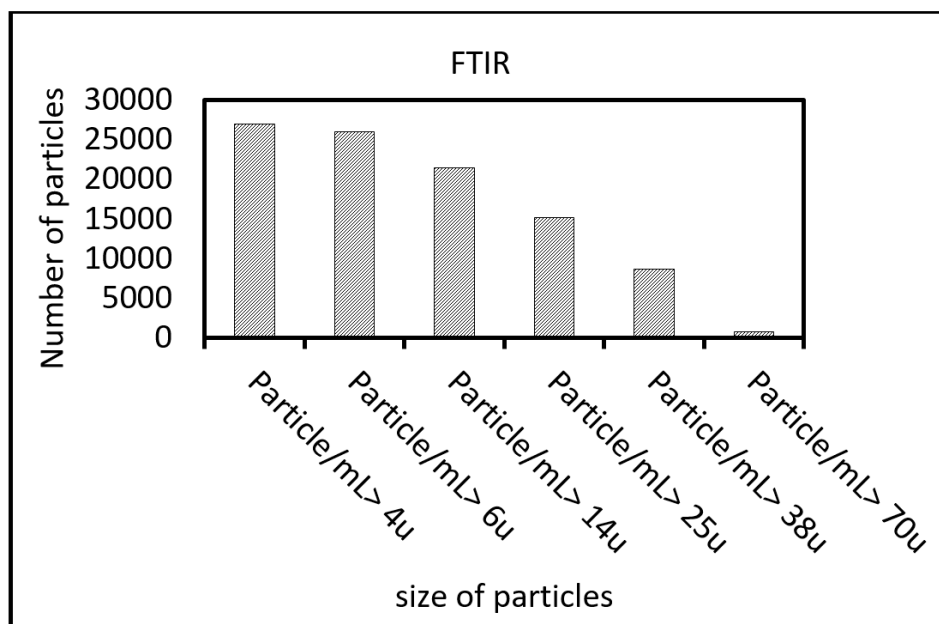

Figure 4. Fourier transform infrared spectroscopy of rGO (error: ±5% according to the manufacturer specification).

To characterize the chemical composition of reduced graphene oxide in terms of its graphitic nature, size of crystalline and structural disorder, Raman spectroscopy was conducted. A 514 nm laser spectra was used to obtain D, G, 2D, and D+D' bands using monochromatic light. From past research, the D band indicates defects in the domain, where increasing the intensity of the D band leads to the formation of more sp2 lattices because of oxidation. The G band stands for the first order dispersion of E2g phonon, which increases C–C tangential vibration or stretching [14]. The ratio of the D band over the G band is crucial to identify defects in the graphitic structure. As shown in Figure 5, Raman spectra

show the D band at 1357 cm^{-1} and the G band at 1601 cm^{-1}. The intensity ratio of the D band and the G band (ID/IG) represent the lattice size. A higher ratio leads to bigger lattice size and as the size of the lattice increases, defects of the sp2 carbon domain. However, for rGO this ratio was found as 0.84, which is low enough to have fewer domain defects [23,27]. The 2D peak is attributed to the number of layers in reduced graphene oxide. In the spectra, the 2D peak attributed at 1845 cm^{-1} and D+G peak at 3178 cm^{-1}. Reduction also increases the intensity of the 2D peak, and as shown in the spectra, the 2D peak intensity was found to be greater, which illustrates that rGO was highly reduced [23,28]. As explained, rGO is hydrophobic and does not allow more oxygen groups between the layers, which enables it to generate gaps between the layers and frictionless conduits in the microstructure. Further, it can accommodate liquid lubricants between the layers. It has been found that mechanical, tensile, and compressive strength are directly proportional to the degree of reduction. The rGO used in this study was highly reduced, which leads to great mechanical, and tensile and compression strength [23]. This is very important for rGO nano additives to mitigate metal-to-metal contact and enhance wear preventive properties.
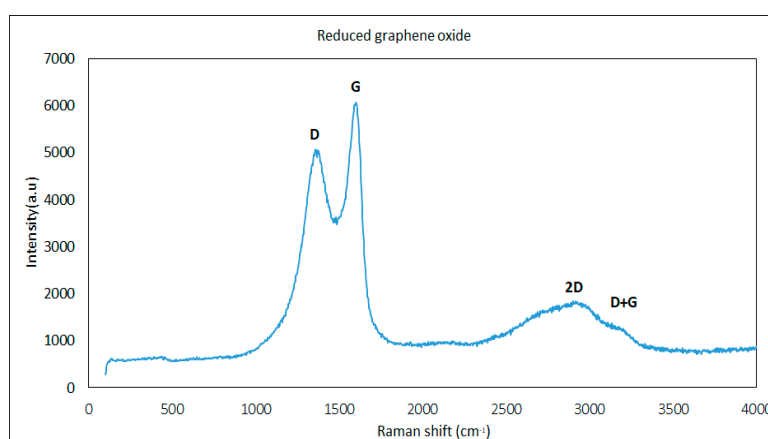

Figure 5. Raman shift (cm^{-1}) of reduced graphene oxide D band, G band, 2D band, and D+D' band.

To provide fault-free machine life, estimation of anti-oxidation capability of lubricants can be investigated using numerous methods such as FTIR, RPVOT, odor, and color inspection. Among these methods, RPVOT is widely used by industry to identify the antioxidant capability of a lubricant [29]. While transforming graphene oxide into its reduced form, there are always a small number of oxygen groups that remain in the lattice, and to understand the effect on anti-oxidation capability because of those oxygen particles, an RPVOT test was conducted as per ASTM D2272 standards. As shown in Table 3, pressure drop time is noted as 27.1, 26.1, 25.8, and 25.7 minutes for pure oil and all three samples, respectively. Comparative studies indicate that there is no noticeable change in anti-oxidation life of all three samples having nano additives compared to the pure oil.

Table 3. Oxidation time of each sample in minutes (error: $\pm5\%$).

Samples	RPVOT in min.
P.O.	27.1
S-1	26.1
S-2	25.8
S-3	25.7

To evaluate the effect of the temperature fluctuation of the pure oil due to the rGO nano additive, a kinematic viscosity test was performed at 40 °C and 100 °C, as per ASTM D445 standards. As shown in Table 4, viscosity at 40 °C and 100 °C are 41.5 mm^2/s and 6.3 mm^2/s, respectively, for the pure oil.

For the other three samples, viscosity is around 41.2 mm^2/s and 6.4 mm^2/s which indicates a negligible decrease in viscosity at lower temperatures and insignificant increase at higher temperatures.

Table 4. Kinematic viscosity and viscosity index at 40°C and 100°C for pure oil and three samples (error: $\pm$ 0.1).

Samples	Viscosity at 40 °C	Viscosity at 100 °C	Viscosity Index
PO	41.5 mm^2/s	6.3 mm^2/s	98
S-1	41.2 mm^2/s	6.4 mm^2/s	104
S-2	41.2 mm^2/s	6.4 mm^2/s	104
S-3	41.2 mm^2/s	6.38 mm^2/s	103

The viscosity index was calculated to investigate the change in viscosity with respect to temperature. Results show that for pure oil, the index was around 98, and for nano lubricants it was 104 at lower concentrations (S-1 and S-2), which reduced to 103 for the more highly concentrated sample (S-3). To recapitulate, the rGO nano lubricant's low viscosity and higher viscosity index enhance shear thinning at solid point contact and reduce frictional losses.

Friction and wear tests were performed in situ to examine the friction behavior of lubricants before adding nano additives to the pure oil, and after adding nano additives at the three concentrations. To obtain precise friction coefficients, data points were taken at 20 ms time intervals. As shown in Figure 6, the friction coefficient for pure oil reduced for fewer revolutions where the rotating speed was low; however, as speed increased logarithmically with the number of revolutions, friction went up and then normalized around 0.2. In the case of S-1 and S-3, the study found the same trend, where friction increased at fewer revolutions and then normalized around 0.3 and 0.35 respectively. The reason behind this could be that S-1 had an uneven rGO nano lubricant film. For S-3, higher conglomerations of the particles might have created a wall at the joint, which can reduce the circulation of lubricant. However, S-2 shows a different trend where friction increased a bit at low speed and revolutions but started normalizing closer to 0.1 at higher speed and revolutions.
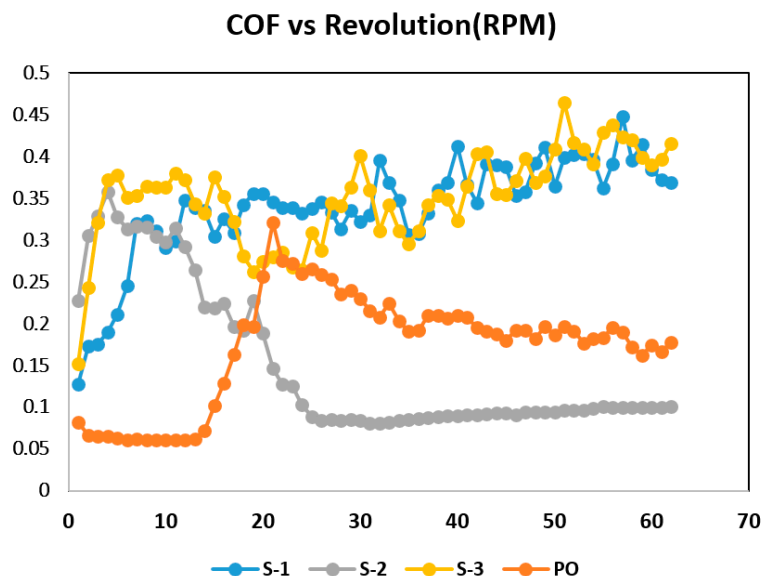

Figure 6. Friction coefficients of pure lubricant and three different samples at 0.01 wt % concentration, 0.05 wt % concentration (grey), and 0.1 wt % concentration.

To understand the wear mechanism of the disk under different lubricants, the wear track of the disk was further studied using hole area analysis, scanning electron microscopy (SEM), and optical profilometer. As shown in Figure 7, the wear rate for the pure oil was calculated as

48.33×10^{-5} mm^3/Nm which is comparatively higher than the other three nano lubricants. S-1 reduced wear by 22.06%, S-2 by 51.85% and S-3 by 25.64% in comparison to the pure oil, which allows the lubricant to enhance tribological surfaces.
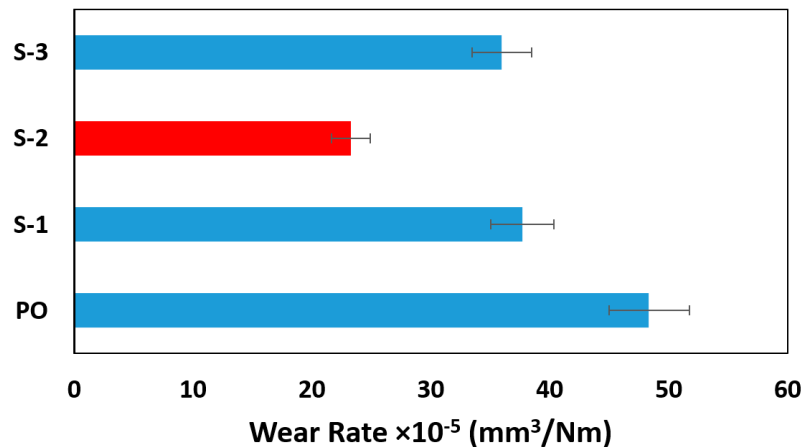

Figure 7. Wear rate for pure oil and three nano lubricants.

Figure 8 shows the schematic view of the interaction of ball, disk, and nano additives used for these experiments to understand the behavior of nano particles under the test conditions. For S-1, only 0.01 wt % nano additives were amalgamated into the pure oil, which indicates low wear compared to pure oil due to penetration of rGO platelets in the contact regime. In the case of S-2, 0.05 wt % nano additives were mixed into the pure oil, which showed the lowest wear among all four samples as well as a reduction in friction after a perfectly hydrodynamic condition was achieved. This allows the lubricant to mitigate metal-to-metal contact, which can be considered as optimal concentration. On the other hand, in S-3, 0.1 wt % concentration was prepared, which led to reduction in wear; however, friction for this sample was highest. This can be due to a high concentration rGO nano platelets starting to conglomerate around the contact patch. Conglomerated nano platelets will generate lower suspension and will inhibit the rGO nano platelets from entering into the patch; but due to high concentration and lower viscosity it will require more energy, which can result in increasing friction. Conversely, some particles will enter the tribo contact and shear the rGO layer, which helps to reduce wear compared to the base oil.
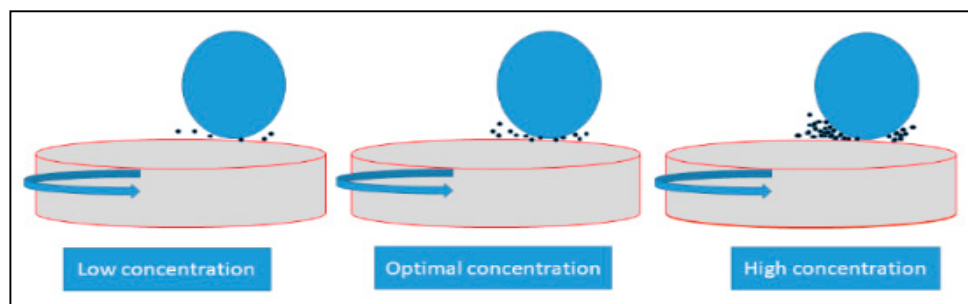

Figure 8. Schematic image showing rGO nano particles in the contact patch at different concentrations.

The wear of the disks is affected by a number of factors, such as the concentration of the additive rGO, contact stress, mechanical properties of the material, temperature, and surface-moving speed, etc. The beneficial effect of adding rGO nano platelets on wear can be justified from the performance of the disk under different rGO concentration.

Wear tracks for all four disk samples were investigated at 500 μm and 120× magnification, as shown in Figure 9. At high magnification, worn material debris was investigated on the wear track

for all four samples. There are some deep grooves on the worn surface of the pure oil (control sample) and S-1 and the width of the wear scars are about 890 μm and 746 μm, respectively. Both control sample (pure oil) and low rGO sample (S-1) suffered severe wear and the deep grooves are parallel with the sliding direction. The wear mechanism can be adhesive wear. Sample-2 (S-2) shows a smooth wear track (605 μm) which does not have any deep scratches, significant plastic deformation, or deep sliding direction marks. The rGO nano platelets in S-2 reduce friction by preventing sliding contact interfaces from severe or more frequent metal-to-metal contacts. By increasing the rGO concentration in S-3, the rGO nano platelets agglomerated together to form abrasive particles which resulted in increasing the width of the wear scar for S-3 to 709 μm. In the future of this study, further theoretical and experimental analysis need to be conducted to investigate the mechanism of wear at different concentration of nano additives (rGO).
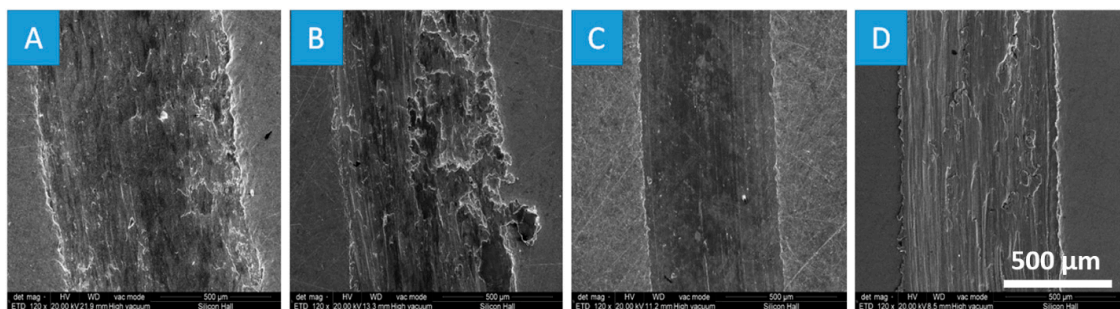

Figure 9. Morphology investigation under scanning electron microscopy (SEM: secondary electron (SE)) of specimen wear tracks at different 500 μm and 120× for pure oil (**A**), S-1 (**B**), S-2 (**C**), and S-3 (**D**).

Profilometry data was obtained in situ to understand the effect of nano lubricants on surface roughness using a non-contact type optical probe. ISO 25178 was used to obtain height parameters such as Sa (arithmetic mean height of the scar) and Sz (maximum height of surface). As shown in Table 5, pure oil has an arithmetic mean height of 1.386 μm and the maximum height of the surface is 15.19 μm, compared to that of S-2, which has an arithmetic mean height of 0.6091 μm and the maximum height of the surface is 11.89 μm, which leads us to conclude that, except for S-2, all three samples, including pure oil, have high adhesive wear.

Table 5. Height parameters of the scar after performing ball-on-disk test.

Samples	Sa (μm)	Sz (μm)
PO	1.386 ± 0.0693	15.19 ± 0.0035
S-1	2.018 ± 0.1009	25.67 ± 0.0050
S-2	0.6091 ± 0.0305	11.89 ± 0.0015
S-3	1.995 ± 0.0998	37.55 ± 0.0050

4. Conclusions

In this research, a novel application of reduced graphene oxide as a friction modifier and wear-resistive nano additive was evaluated. Findings of physical properties have proven that due to nano additives, viscosity negligibly changed for all samples compared to pure oil. On the other hand, anti-oxidation capabilities of the lubricant are not compromised by nano additives, ensuring the same lubrication life. S-1 (0.01% w/w), S-2 (0.05% w/w) and S-3 (0.1% w/w) reduced wear rate by 22.06%, 51.85% and 25.64%, respectively, compared to pure oil. This is very promising for prolonging the life of contact surfaces. In addition, less wear allows industries to use the same contact surfaces longer than their original life cycles. In addition, FTIR particle counting results found that most of the additives of rGO were smaller than 30 μm, which allows this lubricant to be used in diverse applications without damaging filters. As carbon is easily available in the market and manufacturing of reduced graphene

oxide can be easily scaled for industrial demand, it can be efficiently introduced to the next generation of lubricants. For future work, this additive should be tried with different tribology modifiers to determine the effects of more than two additives on the lubricants.

References

1. Holmberg, K.; Erdemir, A. Influence of tribology on global energy consumption, costs and emissions. *Friction* **2017**, *5*, 263–284. [CrossRef]
2. Hutchings, I.; Shipway, P. *Tribology: Friction and Wear of Engineering Materials*; Butterworth-Heinemann: Oxford, UK, 2017.
3. Padgurskas, J.; Rukuiza, R.; Prosyčevas, I.; Kreivaitis, R. Tribological properties of lubricant additives of fe, cu and co nanoparticles. *Tribol. Int.* **2013**, *60*, 224–232. [CrossRef]
4. Cho, D.-H.; Kim, J.-S.; Kwon, S.-H.; Lee, C.; Lee, Y.-Z. Evaluation of hexagonal boron nitride nano-sheets as a lubricant additive in water. *Wear* **2013**, *302*, 981–986. [CrossRef]
5. Lee, J.; Cho, S.; Hwang, Y.; Lee, C.; Kim, S.H. Enhancement of lubrication properties of nano-oil by controlling the amount of fullerene nanoparticle additives. *Tribol. Lett.* **2007**, *28*, 203–208. [CrossRef]
6. Mauter, M.S.; Elimelech, M. Environmental applications of carbon-based nanomaterials. *Environ. Sci. Technol.* **2008**, *42*, 5843–5859. [CrossRef] [PubMed]
7. Geim, A.K.; Novoselov, K.S. The rise of grapheme. In *Nanoscience and Technology: A Collection of Reviews from Nature Journals*; World Scientific: Singapore, 2010; pp. 11–19.
8. Stankovich, S.; Dikin, D.A.; Dommett, G.H.; Kohlhaas, K.M.; Zimney, E.J.; Stach, E.A.; Piner, R.D.; Nguyen, S.T.; Ruoff, R.S. Graphene-based composite materials. *Nature* **2006**, *442*, 282–286. [CrossRef]
9. Geim, A.K.; Novoselov, K.S. The rise of grapheme. *Nat. Mater.* **2007**, *6*, 183–191. [CrossRef]
10. Balandin, A.A.; Ghosh, S.; Bao, W.; Calizo, I.; Teweldebrhan, D.; Miao, F.; Lau, C.N. Superior thermal conductivity of single-layer grapheme. *Nano Lett.* **2008**, *8*, 902–907. [CrossRef]
11. Lee, C.; Wei, X.; Kysar, J.W.; Hone, J. Measurement of the elastic properties and intrinsic strength of monolayer grapheme. *Science* **2008**, *321*, 385–388. [CrossRef]
12. Orlita, M.; Faugeras, C.; Plochocka, P.; Neugebauer, P.; Martinez, G.; Maude, D.K.; Barra, A.-L.; Sprinkle, M.; Berger, C.; De Heer, W.A.; et al. Approaching the dirac point in high-mobility multilayer epitaxial grapheme. *Phys. Rev. Lett.* **2008**, *101*, 267601. [CrossRef]
13. Service, R.F. Materials science. Carbon sheets an atomthick give rise to graphene dreams. *Science* **2009**, *324*, 875–877. [CrossRef] [PubMed]
14. Kim, H.J.; Lee, S.-M.; Oh, Y.-S.; Yang, Y.-H.; Lim, Y.S.; Yoon, D.H.; Lee, C.; Kim, J.-Y.; Ruoff, R.S. Unoxidized graphene/alumina nanocomposite: Fracture-and wear-resistance effects of graphene on alumina matrix. *Sci. Rep.* **2014**, *4*, 5176. [CrossRef] [PubMed]
15. Wu, Z.-S.; Ren, W.; Gao, L.; Liu, B.; Jiang, C.; Cheng, H.-M. Synthesis of high-quality graphene with a pre-determined number of layers. *Carbon* **2009**, *47*, 493–499. [CrossRef]
16. Zhong, Y.L.; Tian, Z.; Simon, G.P.; Li, D. Scalable production of graphene via wet chemistry: Progress and challenges. *Mater. Today* **2015**, *18*, 73–78. [CrossRef]
17. Lu, G.; Ocola, L.E.; Chen, J. Gas detection using low-temperature reduced graphene oxide sheets. *Appl. Phys. Lett.* **2009**, *94*, 083111. [CrossRef]
18. Wang, S.J.; Geng, Y.; Zheng, Q.; Kim, J.-K. Fabrication of highly conducting and transparent graphene films. *Carbon* **2010**, *48*, 1815–1823. [CrossRef]
19. Becerril, H.A.; Mao, J.; Liu, Z.; Stoltenberg, R.M.; Bao, Z.; Chen, Y. Evaluation of solution-processed reduced graphene oxide films as transparent conductors. *ACS Nano* **2008**, *2*, 463–470. [CrossRef]

20. Yang, D.; Velamakanni, A.; Bozoklu, G.; Park, S.; Stoller, M.; Piner, R.D.; Stankovich, S.; Jung, I.; Field, D.A.; Ventrice, C.A., Jr.; et al. Chemical analysis of graphene oxide films after heat and chemical treatments by x-ray photoelectron and micro-raman spectroscopy. *Carbon* **2009**, *47*, 145–152. [CrossRef]

21. Gómez-Navarro, C.; Weitz, R.T.; Bittner, A.M.; Scolari, M.; Mews, A.; Burghard, M.; Kern, K. Electronic transport properties of individual chemically reduced graphene oxide sheets. *Nanoletters* **2007**, *7*, 3499–3503. [CrossRef]

22. Lee, S.W.; Mattevi, C.; Chhowalla, M.; Sankaran, R.M. Plasma-assisted reduction of graphene oxide at low temperature and atmospheric pressure for flexible conductor ap-plications. *J. Phys. Chem. Lett.* **2012**, *3*, 772–777. [CrossRef]

23. Cheng, M.; Yang, R.; Zhang, L.; Shi, Z.; Yang, W.; Wang, D.; Xie, G.; Shi, D.; Zhang, G. Restoration of graphene from graphene oxide by defect repair. *Carbon* **2012**, *50*, 2581–2587. [CrossRef]

24. Hazra, K.; Rafiee, J.; Rafiee, M.; Mathur, A.; Roy, S.; McLauhglin, J.; Koratkar, N.; Misra, D. Thinning of multilayer graphene to monolayer graphene in a plasma environment. *Nanotechnology* **2010**, *22*, 025704. [CrossRef] [PubMed]

25. Eda, G.; Chhowalla, M. Chemically derived graphene oxide: Towards large-area thin-film electronics and optoelectronics. *Adv. Mater.* **2010**, *22*, 2392–2415. [CrossRef] [PubMed]

26. Zaaba, N.; Foo, K.; Hashim, U.; Tan, S.; Liu, W.-W.; Voon, C. Synthesis of graphene oxide using modified hummers method: Solvent influence. *Procedia Eng.* **2017**, *184*, 469–477. [CrossRef]

27. Hafiz, S.M.; Ritikos, R.; Whitcher, T.J.; Razib, N.M.; Bien, D.C.S.; Chanlek, N.; Nakajima, H.; Saisopa, T.; Songsiriritthigul, P.; Huang, N.M.; et al. A practical carbon dioxide gas sensor using room-temperature hydrogen plasma reduced graphene oxide. *Sens. Actuators B Chem.* **2014**, *193*, 692–700. [CrossRef]

28. Shahriary, L.; Athawale, A.A. Graphene oxide synthesized by using modified hummers approach. *Int. J. Renew. Energy Environ. Eng.* **2014**, *2*, 58–63.

29. Sitton, A.; Ameye, J.; Kauffman, R.E. Residue analysis on RPVOT test samples for single and multiple antioxidants chemistry for turbine lubricants. *J. ASTM Int.* **2006**, *3*, 1–15. [CrossRef]